Multimodality imaging of coronary artery bypass grafts

Salm, L.P.

CHAPTER 2

Cardiovascular magnetic resonance and computed tomography of coronary artery bypass grafts

Liesbeth P. Salm
Jeroen J. Bax
Joanne D. Schuijf
Hildo J. Lamb
J.Wouter Jukema
Ernst E. van der Wall
Albert de Roos

Chapter 21 in: MRI and CT of the cardiovascular system. Second edition.
Lippincott Williams & Wilkins 2005

INTRODUCTION

Coronary artery bypass grafting (CABG) is a commonly performed surgical procedure for alleviation of symptoms and prolonging survival for patients with ischemic heart disease. Bypass graft disease is a common consequence, requiring x-ray coronary angiography for diagnosis. Coronary angiography is an invasive procedure that includes x-ray exposure, hospitalization, and a small risk of complications, including arrhythmias, coronary artery dissection, and cardiac death. A noninvasive diagnostic method for the assessment of bypass graft anatomy and function is of great benefit. This chapter reviews the research that has been performed in evaluating bypass grafts noninvasively using cardiovascular magnetic resonance (CMR) and computed tomography (CT).

CARDIOVASCULAR MAGNETIC RESONANCE OF CORONARY ARTERY BYPASS GRAFTS

Anatomy Assessment: Angiography

During the past decades, a considerable amount of effort has been invested to achieve noninvasive visualization of the coronary arteries and bypass grafts with CMR. The relatively larger size, straight course, and immobility during the cardiac cycle of coronary bypass grafts allowed the evaluation of graft patency even in the earliest studies, whereas assessment of the coronary arteries could not be achieved at that stage. In these initial investigations, two-dimensional (2D) spin-echo and gradient-echo techniques were

Author	Patients	Grafts	Graft type	Magnetic resonance technique	Assessable grafts (%)	Sensitivity (%)	Specificity (%)
White et al (4)	25	72	vein	2-D SE	90	72	91
Rubinstein et al (6)	20	47	vein	2-D SE	100	72	90
Jenkins et al (3)	22	45	vein	2-D SE	100	73	89
Frija et al (2)	28	52	vein and arterial	2-D SE	100	71	97
White et al (5)	10	28	vein and arterial	2-D GE	100	86	93
Aurigemma et al (1)	20	45	vein and arterial	2-D GE	100	100	88
Vanninen et al (7)	8	8	GEA	2-D GE	100	100	100
Galjee et al (8)	47	84	vein	2-D SE	92	84	98
				2-D GE	92	88	98
Weighted Mean 2D					95	81	94
Kessler et al (11)	8	21	vein and arterial	3-D NAV	90	100	87
Engelmann et al (9)	16	55	vein and arterial	3-D CE	100	85	95
Vrachliotis et al (14)	15	45	vein and arterial	3-D CE	98	93	97
Wintersperger et al (15)	27	76	vein and arterial	3-D CE	100	81	95
Kalden et al (10)	22	59	vein and arterial	3-D CE	100	93	93
Molinari et al (13)	18	51	vein and arterial	3-D NAV	96	92	97
Langerak et al (12)	38	56	vein	3-D NAV	100	83	98
Wittlinger et al (16)	34	82	vein and arterial	3-D NAV	90	78	96
Bunce et al (17)	34	79	vein and arterial	3-D CE	100	73	85
Weighted Mean 3D					96	85	94

SE = spin-echo; GE = gradient-echo; GEA = gastroepiploic artery; NAV = navigator; CE = contrast-enhanced

Table 2.1

Detection of occlusion in vein and arterial grafts by magnetic resonance angiography compared with invasive angiography

applied to acquire successive axial slices during repetitive breath-holds (1-8). With the spin-echo technique, absence of signal at different levels was considered to indicate the presence of a patent graft because in normal grafts, rapid blood movement is present. To obtain adequate contrast, however, sufficient flow between the graft lumen and the wall is needed, whereas the presence of metallic clips, stents, or calcifications may result in a signal void that can be mistaken for graft stenosis or occlusion. In contrast, flowing blood is depicted as a bright signal during imaging with gradient MR techniques. As shown in Table 2.1, both acquisition techniques have been evaluated in several studies with conventional angiography as the standard of reference, demonstrating sensitivities and specificities varying from 71% to 100% and 89% to 100%, respectively. Pooled analysis of these eight studies (with 180 patients and 381 grafts) revealed a weighted mean sensitivity and specificity of 81% and 94%, with inclusion of 95% of grafts. Despite these promising results in the distinction between patent and occluded grafts, these 2D techniques were still limited by their low signal-to-noise ratio and low spatial resolution. Substantial progress in image quality was achieved by the development of three-dimensional (3D) imaging techniques, allowing the acquisition of volume slabs containing several thin slices and imaging with high spatial resolution. To improve patient comfort, navigator techniques have been developed that permit real-time monitoring of diaphragm motion and thus free-breathing during data acquisition. In addition, improved enhancement of blood/muscle contrast can be expected by the administration of intravascular contrast agents. An example of a typical MR acquisition protocol with navigator respiratory gating is depicted in Figure 2.1. In Figure 2.2 a resulting 3D reconstruction is shown, and an example of a patent bypass graft as confirmed by conventional angiography is provided in Figure 2.3.

Pooled analysis of nine studies using 3D techniques, with more than 200 patients included, revealed a slight increase in weighted sensitivity from 81% to 85%, with no loss in specificity (Figure 2.4) (9-17). Sensitivity and specificity for the different types of grafts (as reported in seven studies) are shown in Figure 2.5. No difference in diagnostic accuracy for detection of graft occlusion was noted between arterial and vein grafts. In particular, the sensitivity and specificity of arterial grafts were 85% and 95% compared with 86% and 93% in vein grafts (9;10;12-14;16;17). These studies illustrate the potential of CMR to evaluate graft patency in clinical routine. Its safe and noninvasive nature in combination with the high specificity (~94%) and negative predictive value (~96%) suggests that in patients presenting with recurrent symptoms after bypass grafting, CMR may function as a first-line investigation tool to rule out graft occlusion before more invasive diagnostic procedures.

However, few attempts thus far have been made to evaluate graft stenosis in addition to assessment of patency. Langerak and colleagues observed a sensitivity and specificity of 82% and 88% for the detection of ≥50% luminal narrowing in vein bypass grafts (12). In contrast, a discouraging sensitivity of 38% was reported by Kalden et al. (10). Because the presence of graft stenosis rather than total occlusion of the graft may be the cause of recurrent complaints, the value of MR angiography (MRA) to evaluate graft stenosis needs to be further explored before routine use of the technique is feasible. In addition, recurrent anginal complaints may also be attributable to progression of coronary artery

disease in native coronary vessels, and assessment in these vessels is still severely hampered by the current spatial and temporal resolution. A possible solution to this limitation may lie in the combination of MRA with MR flow mapping, since the latter provides a functional measurement of the entire vascular tree beyond the level of the flow measurement. Moreover, because the functional graft status is not directly related to the degree of luminal narrowing, improved diagnostic accuracy and management may be expected by such a combined approach.

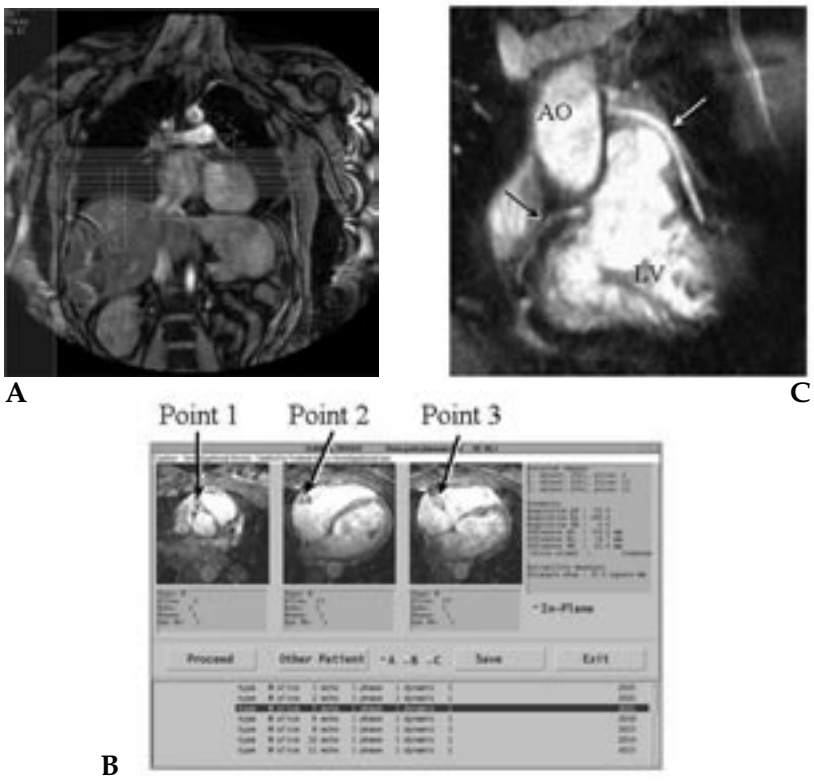

Figure 2.1

Typical magnetic resonance (MR) acquisition protocol. (A) Typical plan-scan for cardiovascular magnetic resonance (CMR) angiography. Axial imaging volume (horizontal lines); volume used for localized shimming (large box); position in the right hemidiaphragm of the respiratory navigator (rectangular box); position of a saturation band for suppression of image artifacts (left box). (B) With the use of axial scout images, the three-point plan-scan is used to select three points in space, one at the origin of the coronary artery or bypass graft, one at the most distal point, and one in the middle of the first two points. From this information, an imaging plane is automatically calculated in plane with the coronary artery or bypass graft of interest. (C) CMR angiography of a patient with a bypass of the left coronary system (white arrow) and a visible native right coronary artery (black arrow). This imaging approach can be used clinically to assess bypass graft patency. AO = aorta; LV = left ventricle. (Courtesy of H.J. Lamb) A full colour version of this illustration can be found in the full colour section (page 164).

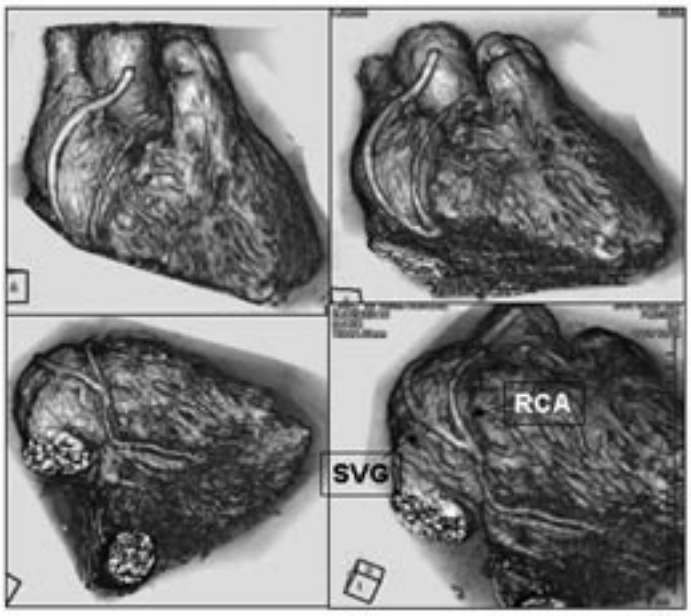

Figure 2.2
Whole-heart CMR angiography of a vein bypass graft to the right coronary artery at different rotation angles. (Courtesy of Dr. H. Sakuma) A full colour version of this illustration can be found in the full colour section (page 165).

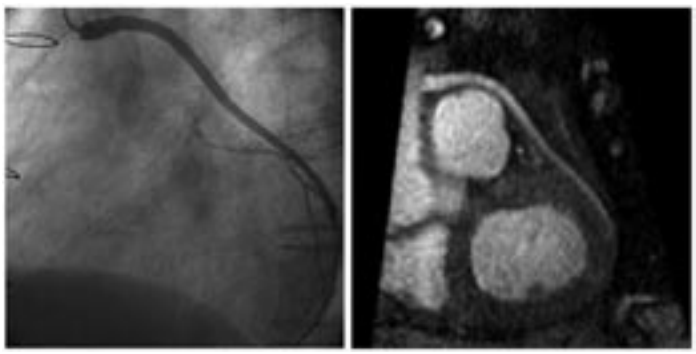

Figure 2.3
MR angiogram of a vein graft (right) in comparison with a coronary angiogram (left). Multiplanar reformat reconstruction is shown of a free-breathing, three-dimensional (3D), navigator-gated sequence used for acquisition of the MR angiogram.

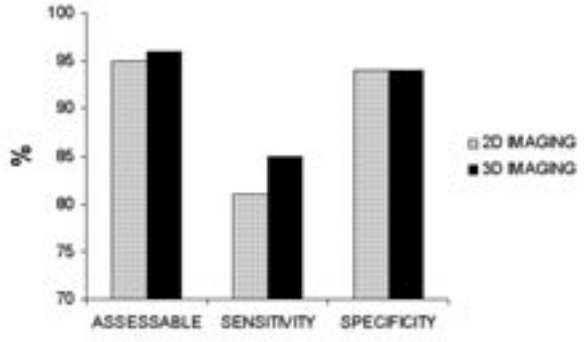

Figure 2.4
Sensitivities and specificities of two-dimensional (2D) and 3D MR angiography (MRA) acquisition techniques (data based on references 1-17).

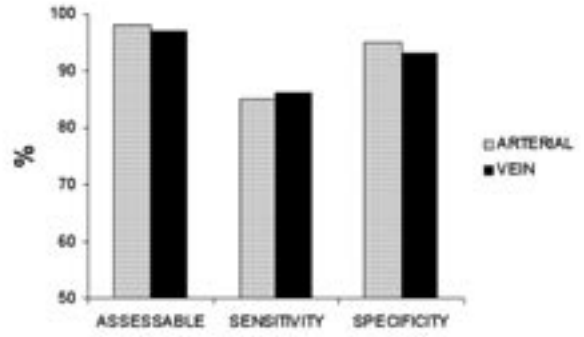

Figure 2.5
Performance of 3D MRA in arterial and vein grafts (data based on references 9,10,12-14,16,17).

Functional Assessment: Flow Velocity
A vessel narrowing, visualized by means of angiography, may or may not impair flow through that vessel (18;19). The assessment of blood flow through coronary arteries and bypass grafts has gained wide attention. To evaluate the hemodynamic impairment of a lesion, flow is measured at rest and during pharmacologically induced stress, for instance with adenosine or dipyridamole (20). By dividing the flow value during stress by the flow value at rest, the coronary flow reserve (CFR) is calculated (21;22). Flow-limiting stenoses cause a compensatory vasodilatation at rest to maintain sufficient blood flow to the myocardium. As a consequence, the vessel cannot respond adequately to an increase in absolute blood flow by vasodilatation during pharmacologically induced stress, and CFR will be reduced. At first, blood flow was determined by means of Doppler flow transducers at open-chest procedures (18;21-25), limitating extensive use

of CFR in clinical practice. When the diameter of intravascular catheter-based Doppler ultrasonographic devices could be reduced to 0.018 inch, it became feasible to measure the velocity of the blood flow and calculate the coronary flow velocity reserve (CFVR) for coronary arteries in patients during catheterization. Blood flow correlated well with Doppler-derived velocity of blood flow both in vitro and in vivo (26-28). Invasive Doppler-derived CFVR has proven its potential in numerous clinical applications, such as in identifying hemodynamic significant stenoses in native coronary arteries and vein grafts (29;30), in the functional assessment of stenoses of intermediate severity (31), in the determination of the need for and the outcome after coronary intervention (32-34) and in the prediction of restenosis (35).
With the use of MR, blood flow velocity can be measured using phase-contrast, velocity-encoded sequences (36). To use such a sequence accurately, an imaging plane perpendicular to the target vessel has to be selected by means of survey images. Throughout the cardiac cycle, the acquisition yields anatomic modulus images, paired with phase images, in which every pixel contains a different velocity value. Volume flow (in milliliters/min) can be obtained by calculating the integrated volumetric flow rate of all pixels in the vessel lumen per heartbeat and multiply it with the heart rate. To display the flow pattern, a flow rate-versus-time graph can be presented. Alternatively, the central peak velocity (in centimeters per second) can be obtained by selecting several pixels in the vessel center. Figure 2.6 depicts a typical example of a MR velocity mapping examination in a vein graft.

Early magnetic resonance studies in vein grafts
For vein grafts, feasibility to quantify flow and characterize the flow pattern noninvasively by MR was demonstrated (37;38). To establish feasibility, an attempt to measure flow in 49 vein grafts with ≤50% luminal stenosis at coronary angiography in 27 patients was made (38). In 84% of grafts, flow could be measured adequately. In another early study, 23 vein grafts in 18 patients were studied to distinguish normal from dysfunctional grafts by MR with flow mapping plus coronary angiography as the gold standard (39). They found that graft flow <20 ml/min and a loss of the biphasic flow pattern, typical for bypass grafts, would indicate a dysfunctional graft. On top of comparing spin-echo with cine gradient-echo MR assessment of vein graft patency, Galjee et al. (8) investigated vein graft function by phase-velocity imaging. In 62 of the 73 angiographically patent grafts (85%), adequate biphasic flow profiles could be obtained. A significant difference in flow between single grafts and sequential grafts to three vascular regions was demonstrated. These early vein graft flow studies were limited by the use of a gradient-echo sequence with limited spatial resolution (1.9x1.2x5 mm^3) and no compensation for respiratory motion on 0.5 to 0.6 Tesla (T) magnets.

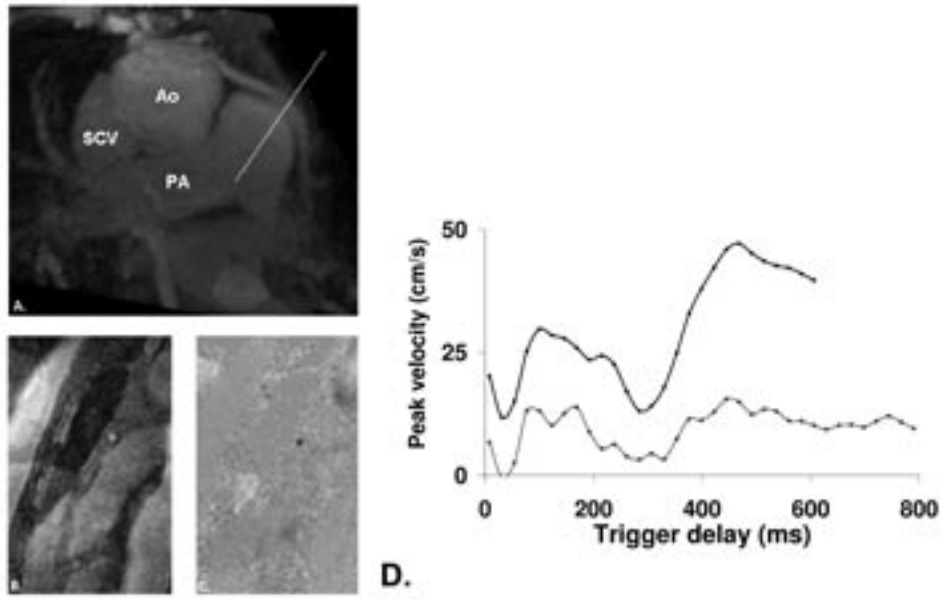

Figure 2.6

MR flow velocity study. Survey image visualizing a vein graft in plane (A). A plane perpendicular to the graft is selected, and modulus and phase images are acquired (B,C). The graft is pictured as a white, respectively black spot in the center of the image. In every image in the cardiac cycle 4 pixels in the center of the graft are selected to obtain a velocity curve (D). The MR flow velocity acquisition is repeated during adenosine-induced stress to obtain the stress velocity curve (black graph). Ao = aorta; PA = pulmonary artery; SCV = supracaval vein.

Early magnetic resonance studies in arterial grafts

Feasibility to quantify flow in native and grafted internal mammary arteries (IMAs) was demonstrated in 10 volunteers and 15 patients using a free-breathing gradient-echo sequence on a 1.5 T MR scanner (40). Patients had recently undergone IMA grafting; no control angiography of the arterial grafts was performed. A large intersubject variation of IMA graft flow (range 28-164 ml/min) was observed. Mean flow and peak velocity were lower in IMA grafts compared with native IMAs. In a different feasibility study, respiratory motion was compensated using a breath-hold segmented k-space gradient-echo sequence to quantify velocity in native and grafted IMAs (41). IMA grafts were investigated within 6 months after CABG; no control angiography was available. Comparison with a free-breathing techique in native IMAs demonstrated a higher peak velocity using the breath-hold sequence because of elimination of respiratory motion artifacts and averaging of velocities. This sequence allowed imaging time to decrease from approximately 4 minutes at free-breathing to a 20-second breath-hold. By means of a view-sharing reconstruction, an effective temporal resolution of 64 ms could be maintained, allowing an acquisition of 7 to 13 temporal phases in a cardiac cycle.

Angiographically controlled magnetic resonance studies in vein and arterial grafts

To evaluate the diagnostic value of MR flow velocity in bypass grafts, several angiographically controlled studies were performed. In addition to investigating the accuracy of contrast-enhanced MRA in the evaluation of bypass grafts postoperatively, Brenner et al. (42) performed additional MR velocity mapping of the grafts. Only 65% of the 247 obtained MR velocity images could be evaluated because of metal clip artifacts in IMA grafts. Concerning the MR velocity measurements, they concluded that this technique was not qualified for the detection of bypass graft stenoses.

With the use of breath-hold sequences, flow measurements at rest and during pharmacologically induced stress with determination of CFR in bypass grafts could be achieved. Langerak et al. (43) validated a breath-hold turbo-field echo-planar imaging sequence by demonstrating a good correlation with a free-breathing technique for aortic and native IMA flow in volunteers. This sequence was subsequently used to measure flow at rest and during adenosine-induced stress in 2 arterial and 18 vein grafts, which were patent at coronary angiography. A significant increase at adenosine-induced stress for flow and velocity parameters was observed, and CFR (mean 2.7 ± 1.1 for single grafts) could be calculated. In another study, MR-derived velocity measurements correlated well with invasive Doppler-derived velocity measurements in 27 grafts (26 vein/1 arterial graft) (44). A significant difference between grafts with <50% stenosis and ≥50% stenosis was demonstrated for MR-derived average peak velocity during adenosine-induced stress (20.2 ± 0.4 vs. 12.2 ± 0.4 cm/s), and diastolic peak velocity during adenosine-induced stress (35.3 ± 0.3 vs. 25.6 ± 0.3 cm/s). Measurements obtained at rest did not show a significant difference between grafts with <50% stenosis and ≥50% stenosis. The detection of ≥70% angiographic stenosis in IMA grafts by breath-hold MR flow velocity at rest and during dipyridamole-induced stress was investigated (45). In 24 early postoperative patients, successful MR flow measurements were performed in the mid-IMA graft. At CABG surgery, titanium clips were used to avoid metal artifacts at MR imaging. A significant difference between grafts with <70% and ≥70% stenosis was demonstrated for baseline mean blood flow (79.8 ± 38.2 ml/min vs. 16.9 ± 5.5 ml/min) and the diastolic-to-systolic velocity ratio (1.88 ± 0.96 vs. 0.61 ± 0.44). Threshold values of 35 ml/min for baseline mean flow and 1.0 for diastolic-to-systolic velocity ratio was proposed to separate IMA grafts with <70% and ≥70% stenosis. Respective sensitivity and specificity were 86% (95% confidence interval [CI]: 49.5-98.7%) and 94% (95% CI: 79.2-99.5%) for the threshold value of baseline mean flow, and 86% (95% CI: 48.6-99.2%) and 88% (95% CI: 72.9-93.8%) for the threshold value of diastolic-to-systolic velocity ratio. CFR did not differ significantly between IMA grafts with <70% and ≥70% stenosis.

The value of MR flow in the prediction of vein graft disease was assessed (46). Forty vein grafts in 21 patients were examined by contrast-enhanced MRA and breath-hold gradient-echo MR flow at rest and during adenosine-induced stress and coronary angiography. An algorithm was formulated combining baseline flow <20 ml/min or CFR<2 to detect grafts or run-offs with a significant stenosis (≥50%) or a myocardial infarction in the graft vascular territory, yielding a sensitivity of 78% with a specificity of 80%. The algorithm was designed to exclude normal-functioning vein grafts from further invasive examinations. A different approach for the detection of stenotic vein and arterial grafts

or recipient vessels by MR with velocity mapping was also developed (47). In this study, 166 grafts were examined by breath-hold MR velocity at rest and during adenosine-induced stress, controlled by coronary angiography. In 80% of grafts full MR examination was successful. Single and sequential vein and arterial grafts were separately analyzed. Marginal logistic regression was used to predict the probability for the presence of ≥50% or ≥70% stenosis per graft type using multiple MR velocity parameters, including CFVR. Sensitivity and specificity for detecting single vein grafts or recipient vessels with ≥50% and ≥70% stenosis were 94% (95% CI: 86-100%) and 63% (95% CI: 48-79%), and 96% (95% CI: 87-100%) and 92% (95% CI: 84-100%), respectively; for detecting ≥50% and ≥70% stenosis in sequential vein grafts these values were 91% (95% CI: 78-100%) and 82% (95% CI: 64-100%), and 94% (95% CI: 83-100%) and 71% (95% CI: 52-91%), respectively. A proposed cut-off point for separating <70% and ≥70% stenosis in single vein grafs was 1.43 for CFVR. Not enough stenoses in arterial grafts were present to formulate an adequate logistic regression model for those grafts.
These studies show that MR flow velocity assessment has high potential to become a valuable, diagnostic tool in predicting patency and even the presence or absence of a significant stenosis in both vein and IMA grafts in clinical practice. Future studies should focus on an integration of bypass graft and native coronary artery MR flow velocity assessment, by which an absence of significant stenosis can be predicted with high accuracy to avoid unnecessary invasive coronary angiographic examinations.

Applied studies using magnetic resonance flow velocity in bypass grafts
Some studies were conducted using MR flow velocity as a tool to evaluate a certain procedure (surgical or percutaneous intervention) or noninvasive modality. Miller et al. (48) used a comprehensive approach of breath-hold contrast-enhanced MRA, non-breath-hold MR flow quantification at rest, and MR cardiac function assessment to evaluate the status of IMA grafts after minimally invasive direct CABG surgery. The protocol was successfully completed in six patients postoperatively. Patency of the grafts was accurately assessed by this MR approach, compared with coronary angiography. To evaluate the value of color-Doppler echography and MRA with navigator-gated flow measurements to assess bypass graft patency postoperatively, a comparison with intraoperative flow measurements was performed (49). Only IMA grafts could be evaluated with color Doppler. They found that both modalities were useful to assess IMA graft patency after surgery, but MR flow measurements had the best correlation with intraoperative flow measurements. In one study, the success of percutaneous interventions in 15 veins was evaluated by breath-hold MR flow, and reference values for rest and adenosine-stress MR flow and velocity parameters were formulated using data of 39 single and 20 sequential vein grafts with <50% stenosis (50). Significant improvements by MR flow after a percutaneous intervention were observed for baseline (before: 9.2 ± 6.6 cm/s; after 12.9 ± 7.9 cm/s) and adenosine-induced stress (before: 12.9 ± 6.3 cm/s; after: 27.1 ± 13.9 cm/s) mean velocity. CFVR did not significantly improve after an intervention (before: 2.4 ± 1.4; after: 2.6 ± 0.9), as a result of an equal recovery of both baseline and stress mean velocity. Reference values confirmed a significant difference between single and sequential vein graft values, underscoring the need to evaluate

these grafts separately. Because a MR velocity map can be analyzed to evaluate both flow and velocity, the diagnostic accuracy of the flow and velocity analysis approach was investigated using velocity maps of 80 single vein grafts (51). A similar diagnostic accuracy was demonstrated for the flow (92%) and velocity analysis (93%) in the detection of ≥70% stenosis. Velocity analysis seemed to be the preferred method, because it is less time-consuming compared with flow analysis.

The functional significance of a bypass graft stenosis was evaluated by single-photon emission computed tomography (SPECT), breath-hold MR velocity at rest and during adenosine-induced stress, and coronary angiography (52). In 18 out of 20 (90%) grafts with a normal myocardial perfusion as determined by SPECT, preserved CFVR (≥2.0) was observed, whereas a reduced CFVR was noted in 19 of 26 grafts (69%) with abnormal perfusion on SPECT. Accordingly, agreement between SPECT perfusion imaging and MR velocity assessment was 80% (κ=0.61). In relation to invasive coronary angiography the following was observed: In grafts with a stenosis <50% and normal perfusion on SPECT, normal CFVR was observed in 86%, whereas reduced CFVR was observed in 78% of grafts with a stenosis ≥50% and abnormal perfusion. All grafts with a stenosis ≥50% and normal perfusion, suggesting no hemodynamic significance of the stenosis, had normal CFVR. Finally, reduced CFVR was observed in 33% of grafts with a stenosis <50% and abnormal perfusion (suggestive of microvascular disease).

Functional Assessment: Left Ventricular Function, Contrast-enhancement, Viability

Few studies have been performed evaluating patients after CABG surgery by a functional MR examination. In one study, global and regional left ventricular (LV) function by 3D MR served as the gold standard for the assessment of LV function by 99m-technetium-sestamibi gated SPECT in patients post-CABG surgery (53). After cardiac surgery, exaggerated systolic anteromedial translation of the entire heart within the chest has been observed, enhancing difficulties in assessing regional wall motion (especially in the septum). They demonstrated that an automated software algorithm (54;55) for the assessment of LV function by SPECT agreed well compared with MR functional assessment in this particular group of patients.

Several studies focused on evaluating myocardial injury by contrast-enhanced MR during off-pump and on-pump CABG surgery. Conventional on-pump surgery uses a cardiopulmonary bypass and aortic cross-clamping, which may lead to a systemic inflammatory response syndrome with multiorgan dysfunction (56) and myocardial damage as the result of ischemia (57). Selvanayagam et al. (58) randomized 60 patients to either off-pump or on-pump CABG surgery and examined those patients before and after surgery by contrast-enhanced MR. Troponin I measurements were also obtained, which correlated with mean mass of new myocardial hyperenhancement. The authors found that off-pump CABG resulted in a significantly better LV function early after surgery; however, it did not reduce the incidence or extent of irreverible myocardial injury. Correlation of elevated biochemical markers (creatinine kinase-MB, troponin I and T) after CABG with the amount of perioperatively infarcted myocardium was confirmed in another study (59). A 6-month follow-up contrast-enhanced MR examination was then performed in the same patient group to assess the diagnostic value of MR contrast

enhancement in predicting viability, and to assess late regional wall motion recovery (60). A strong correlation between the transmural extent of hyperenhancement and regional function recovery at 6 months was demonstrated, revealing contrast-enhanced MR as a powerful predictor of myocardial damage after CABG surgery.

Computed tomography of coronary artery bypass grafts

CT has been intensively investigated in its ability and value to visualize bypass grafts noninvasively. Early studies were using conventional CT scanners to assess bypass graft patency postoperatively, in comparison with coronary angiography. Repeated axial images were acquired at multiple levels of the graft. If the contrast agent was able to visualize the graft at two levels at least, a graft was scored as patent (61;62). This technique required an intravenous bolus of 20 to 50 ml contrast agent per image and therefore burdened the patient with a relatively large quantity of x-ray radiation. Then, CT scanners could be programmed to acquire multiple axial images after one bolus injection of contrast agent (dynamic scanning), allowing faster acquisition of images (63-69). Scans could be repeated after a 1- to 4-second interval, and per bolus injection four to six sequenced scans could be obtained. Diagnostic accuracy for this technique to detect bypass graft patency ranged from 45% to 95%. Ultrafast CT scanning allowed acquisition of one axial image in 50 ms, and repeating of scans after 8 ms (70-72). Total image acquisition time was 10 to 30 heartbeats, using electrocardiograph (ECG) triggering. Sensitivity to detect bypass graft patency using this technique was 93% to 96%, with a specificity of 89% to 100%. With spiral CT scanning the complete heart could be scanned in one breath-hold acquisition of 24 to 30 s (9;73-75). Optimal in-plane spatial resolution using this technique was 0.29 mm^2. Reported diagnostic accuracy for the detection of graft patency was 96% for vein grafts and 88% for arterial grafts (75). Then, it became feasible to use four detectors in a single spiral CT acquisition, allowing detection of graft patency with very high accuracy: 98% to100% for vein grafts and 97% to 100% for arterial grafts (76-82).

Another approach in assessing bypass graft patency is to estimate the graft blood flow. The contrast clearance curve of a contrast bolus injection is evaluated by cine CT (83). This technique was tested in patients, showing a good agreement with observations at coronary angiography (κ=0.75) (84). In addition to assessment of bypass graft patency, the extent of graft disease may be evaluated by CT. With four-detector row CT technology, adequate stenosis assessment of all grafts was prevented by motion artifacts, metal clip artifacts, or beam hardening from calcium deposits (80-82). Table 2.2 shows the percentage of graft segments that could be analyzed and the sensitivity, specificity, and diagnostic accuracy in detecting significant stenoses in patent bypass grafts. Bypass grafts have been examined by 16-detector row spiral CT, allowing a scanning range of the proximal IMA insertion to the heart apex. By using retrospective ECG gating and a segmental reconstruction algorithm, images with an in-plane spatial resolution of up to 0.35 mm^2 can be acquired in a single breath-hold (85-87). In Figure 2.7, a typical 16-slice multislice computed tomography (MSCT) protocol is explained, whereas the different image displays that are available for evaluation of the MSCT angiograms are shown in Figure 2.8.

Author	Patients	Grafts	Graft type	Assessable grafts (%)	Sensitivity (%)	Specificity (%)
Ropers et al (82)	65	124	vein and arterial	62	75	92
Nieman et al (81)	24	39	vein	95	83	90
Marano et al (80)	57	92	vein and arterial	67	80	96
Martuscelli et al (89)	96	278	vein and arterial	88	90	100
Salm et al (87)	25	67	vein and arterial	-	100	95
Weighted Mean		600		80	84	9

Table 2.2

Accuracy of multislice spiral computed tomography in the detection of significant stenoses (≥50% luminal narrowing) in bypass grafts, controlled by coronary angiography

In comparison with coronary angiography, the 16-detector row CT technique was demonstrated to detect bypass graft stenosis of 50% to 100% with a sensitivity of 96% and specificity of 95% (88). In another study, ≥50% angiographic stenoses in patent grafts were detected with a sensitivity of 90% with a specificity of 100% (89). Diagnostic accuracy to detect graft patency was 100%.

Multidetector row CT was used to preoperatively assess the surgical site before totally endoscopic CABG, and the results were correlated with findings at coronary angiography and during surgery (90). Multidetector row CT demonstrated extended information about the coronary target site and is recommended as a planning tool before complex cardiac surgery, such as endoscopic bypass grafting or minimally invasive direct CABG.

Retrospective ECG gating allows reconstruction of CT images at 0% to 90% during the cardiac cycle. The best reconstruction interval to view coronary artery bypass grafts anastomosed to the right coronary artery and branches was shown to be at 50%, whereas grafts anastomosed to the left anterior descending or circumflex artery (or branches) were best viewed at 60% to 70% of the cardiac cycle (79).

As illustrated in Figure 2.9, multidetector row CT (MDCT) technology allows a very accurate evaluation of vein and arterial bypass graft patency. Also, significant stenosis in bypass grafts may be assessed by MDCT. CT technology is rapidly evolving, with 32- and 64-detector row technology being readily available. A simultaneous assessment of native coronary arteries, coronary artery bypass grafts, and recipient vessels noninvasively by MDCT may soon be a part of daily clinical practice.

Summary

CMR and CT have made rapid progress in the last two decades in detecting patency/occlusion and eventually stenoses in coronary artery bypass grafts. Other applications of CMR and CT include pre- and postoperative assessment of the CABG procedure. Future studies should focus on integrating assessment of native coronary arteries and bypass grafts as a full noninvasive evaluation before coronary angiography.

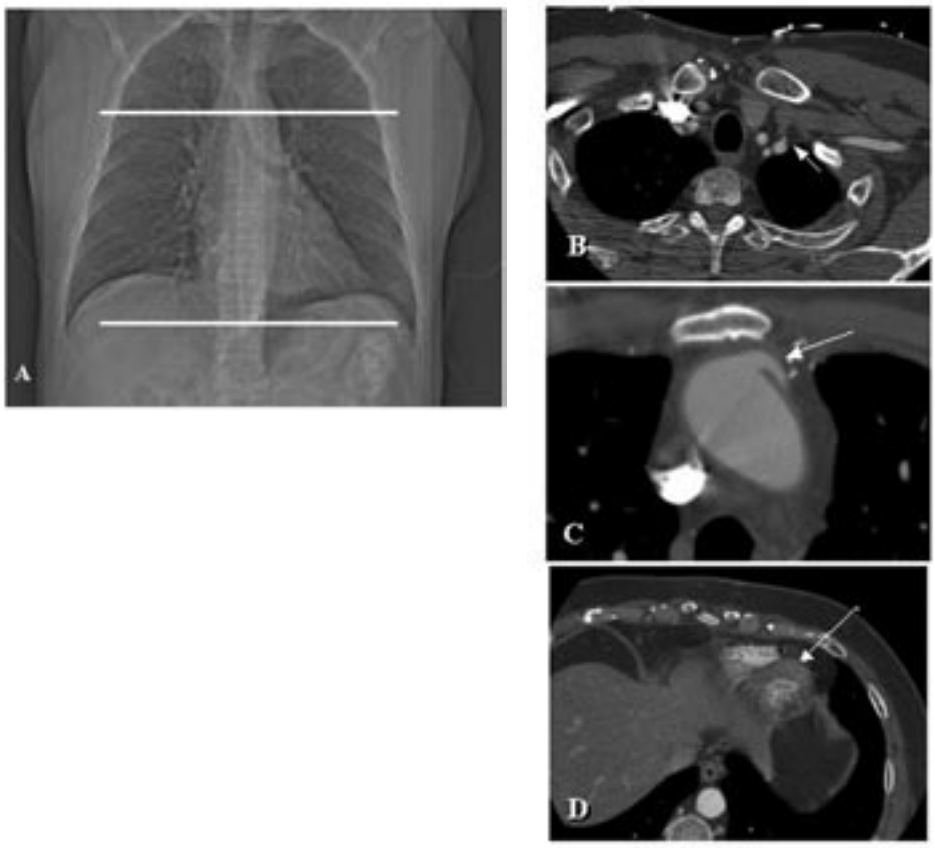

Figure 2.7

Typical 16-slice multislice computed tomography (MSCT) acquisition protocol. Typical coronary computed tomographic angiography (CTA) protocol starts with correct supine patient positioning, positioning of intravenous line, placement of three electrocardiograph (ECG) leads, and patient instruction concerning breath-holding. First, a scanogram for overview is acquired (A). Approximate cranial and caudal imaging margins (white lines) to acquire a second noncontrast localizer with prospective ECG triggering (30-40 slices, 3-mm slice thickness, 120 kV at 200 mA). (B) On the basis of the second localizer, the exact cranial and caudal margins are defined. These margins are depending on the clinical setting, for example, for CTA of arterial graft, such as the left internal mammary artery (IMA) graft, a higher cranial slice is needed (B, arrow) than for CTA of vein grafts (C, arrow). The actual contrast-enhanced helical acquisition should be planned from 1 cm above the defined cranial margin to 1 cm below the caudal margin, i.e. the apex of the heart (D, arrow). For optimal timing of the contrast arrival in the coronary arteries and bypass grafts, automated bolus tracking is applied by placement of a region of interest in the ascending aorta. (continues)

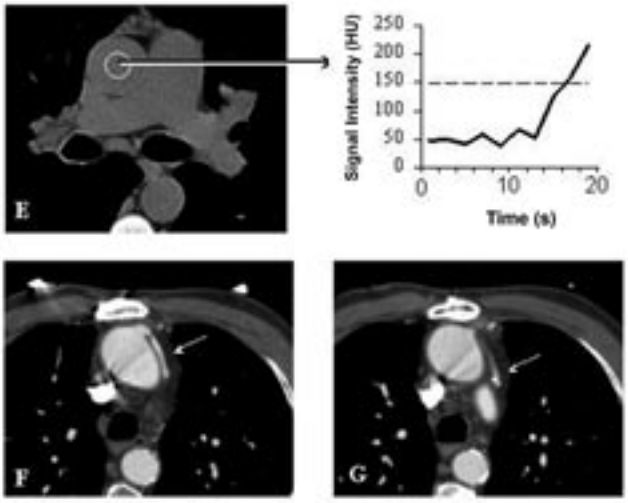

Figure 2.7 (continued)

(E) After the signal intensity reaches a predefined threshold (see graph), the final CTA scan starts automatically. Two levels are shown from the resulting CTA of a vein coronary artery bypass graft (F,G, arrows). CTA was performed with retrospective ECG gating (0.5-mm slice thickness, 120 kV at 250 mA, pitch and rotation time depending on heart rate).

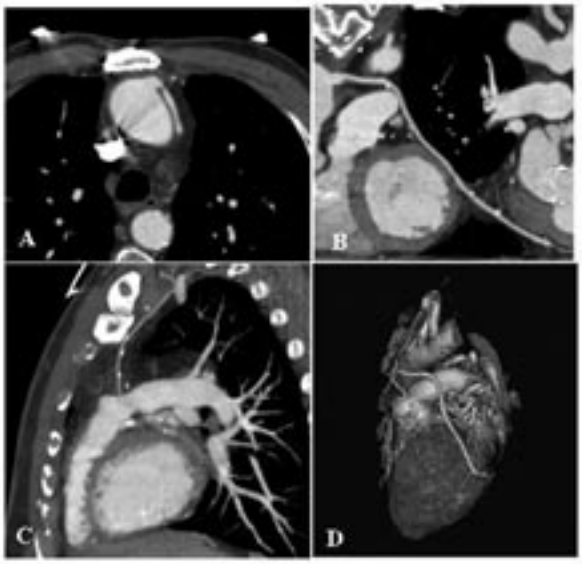

Figure 2.8

For the evaluation of MSCT angiograms, several imaging displays can be used. (A) Original axial slice. (B) Curved multiplanar reconstruction of a vein graft. (C) Maximum intensity projection of an arterial graft. (D) For an overview of the coronary arteries and bypass grafts, 3D volume-rendered reconstructions can be useful. A full colour version of this illustration can be found in the full colour section (page 166).

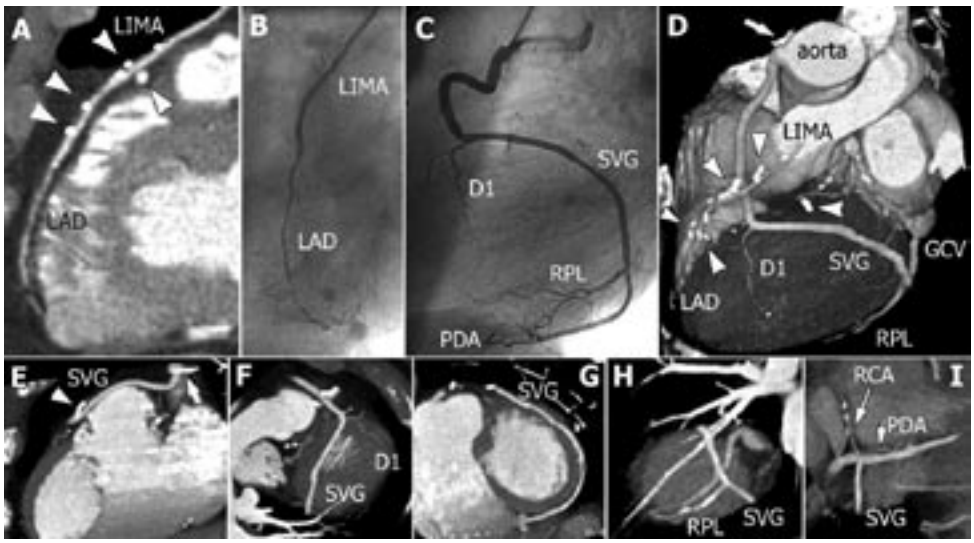

Figure 2.9

Arterial and vein bypass grafts. Images obtained with contrast-enhanced multidetector row CT angiography (A, E-I, maximum intensity projections; D, 3D volume rendering) and corresponding conventional angiography (B,C) show a left IMA graft (LIMA) connected to the left anterior descending coronary artery (LAD). Saphenous vein graft (SVG) runs from the aorta to the diagonal branch (D1), with consecutive jumps to the posterolateral branch (RPL) and posterior descending coronary artery (PDA). Surgical clips (arrowheads) and bypass indicator (arrow in D,E) appear as bright structures. Location of labeled right coronary and posterior descending coronary arteries (arrows in I). GCV = great cardiac vein; RCA = right coronary artery. (Reproduced with permission from Radiology)

References

1. Aurigemma GP, Reichek N, Axel L, Schiebler M, Harris C, Kressel HY. Noninvasive determination of coronary artery bypass graft patency by cine magnetic resonance imaging. Circulation 1989;80:1595-602.
2. Frija G, Schouman Claeys E, Lacombe P, Bismuth V, Ollivier JP. A study of coronary artery bypass graft patency using MR imaging. J Comput Assist Tomogr 1989;13:226-32.
3. Jenkins JP, Love HG, Foster CJ, Isherwood I, Rowlands DJ. Detection of coronary artery bypass graft patency as assessed by magnetic resonance imaging. Br J Radiol 1988;61:2-4.
4. White RD, Caputo GR, Mark AS, Modin GW, Higgins CB. Coronary artery bypass graft patency: noninvasive evaluation with MR imaging. Radiology 1987;164:681-6.
5. White RD, Pflugfelder PW, Lipton MJ, Higgins CB. Coronary artery bypass grafts: evaluation of patency with cine MR imaging. AJR Am J Roentgenol 1988;150:1271-4.
6. Rubinstein RI, Askenase AD, Thickman D, Feldman MS, Agarwal JB, Helfant RH. Magnetic resonance imaging to evaluate patency of aortocoronary bypass grafts. Circulation 1987;76:786-91.
7. Vanninen RL, Vainio PA, Manninen HI, Suhonen M, Jaakola P. Gastroepiploic artery as an in situ coronary artery bypass graft: evaluation of MRI and colour Doppler ultrasound in follow-up. Scand J Thorac Cardiovasc Surg 1995;29:7-10.
8. Galjee MA, van Rossum AC, Doesburg T, van Eenige MJ, Visser CA. Value of magnetic resonance imaging in assessing patency and function of coronary artery bypass grafts. An angiographically controlled study. Circulation 1996;93:660-6.
9. Engelmann MG, Knez A, von Smekal A et al. Non-invasive coronary bypass graft imaging after multivessel revascularisation. Int J Cardiol 2000;76:65-74.
10. Kalden P, Kreitner KF, Wittlinger T et al. Assessment of coronary artery bypass grafts: value of different breath-hold MR imaging techniques. AJR Am J Roentgenol 1999;172:1359-64.
11. Kessler W, Achenbach S, Moshage W et al. Usefulness of respiratory gated magnetic resonance coronary angiography in assessing narrowings > or = 50% in diameter in native coronary arteries and in aortocoronary bypass conduits. Am J Cardiol 1997;80:989-93.
12. Langerak SE, Vliegen HW, de Roos A et al. Detection of Vein Graft Disease using High-resolution Magnetic Resonance Angiography. Circulation 2002;105:328-33.
13. Molinari G, Sardanelli F, Zandrino F, Balbi M, Masperone MA. Value of navigator echo magnetic resonance angiography in detecting occlusion/patency of arterial and venous, single and sequential coronary bypass grafts. Int J Card Imaging 2000;16:149-60.
14. Vrachliotis TG, Bis KG, Aliabadi D, Shetty AN, Safian R, Simonetti O. Contrast-enhanced breath-hold MR angiography for evaluating patency of coronary artery bypass grafts. AJR Am J Roentgenol 1997;168:1073-80.
15. Wintersperger BJ, Engelmann MG, von Smekal A et al. Patency of coronary bypass grafts: assessment with breath-hold contrast-enhanced MR angiography--value of a non-electrocardiographically triggered technique. Radiology 1998;208:345-51.
16. Wittlinger T, Voigtlander T, Kreitner KF, Kalden P, Thelen M, Meyer J. Non-invasive magnetic resonance imaging of coronary bypass grafts. comparison of the haste- and navigator techniques with conventional coronary angiography. Int J Cardiovasc Imaging 2002;18:469-77.
17. Bunce NH, Lorenz CH, John AS, Lesser JR, Mohiaddin RH, Pennell DJ. Coronary artery bypass graft patency: assessment with true ast imaging with steady-state precession versus gadolinium-enhanced MR angiography. Radiology 2003;227:440-6.
18. White CW, Wright CB, Doty DB et al. Does visual interpretation of the coronary arteriogram predict the physiologic importance of a coronary stenosis? N Engl J Med 1984;310:819-24.
19. Topol EJ, Nissen SE. Our preoccupation with coronary luminology. The dissociation between clinical and angiographic findings in ischemic heart disease. Circulation 1995;92:2333-42.
20. Uren NG, Melin JA, De Bruyne B, Wijns W, Baudhuin T, Camici PG. Relation between myocardial blood flow and the severity of coronary-artery stenosis. N Engl J Med 1994;330:1782-8.
21. Gould KL, Lipscomb K, Hamilton GW. Physiologic basis for assessing critical coronary stenosis. Instantaneous flow response and regional distribution during coronary hyperemia as measures of coronary flow reserve. Am J Cardiol 1974;33:87-94.
22. Gould KL, Kirkeeide RL, Buchi M. Coronary flow reserve as a physiologic measure of stenosis severity. J Am Coll Cardiol 1990;15:459-74.
23. Gould KL, Lipscomb K. Effects of coronary stenoses on coronary flow reserve and resistance. Am J Cardiol 1974;34:48-55.

24. Bittar N, Kroncke GM, Dacumos GC, Jr. et al. Vein graft flow and reactive hyperemia in the human heart. J Thorac Cardiovasc Surg 1972;64:855-60.
25. Wilson RF, White CW. Does coronary artery bypass surgery restore normal maximal coronary flow reserve? The effect of diffuse atherosclerosis and focal obstructive lesions. Circulation 1987;76:563-71.
26. Doucette JW, Corl PD, Payne HM et al. Validation of a Doppler guide wire for intravascular measurement of coronary artery flow velocity. Circulation 1992;85:1899-911.
27. Sudhir K, Hargrave VK, Johnson EL et al. Measurement of volumetric coronary blood flow with a Doppler catheter: validation in an animal model. Am Heart J 1992;124:870-5.
28. Labovitz AJ, Anthonis DM, Cravens TL, Kern MJ. Validation of volumetric flow measurements by means of a Doppler-tipped coronary angioplasty guide wire. Am Heart J 1993;126:1456-61.
29. Ofili EO, Labovitz AJ, Kern MJ. Coronary flow velocity dynamics in normal and diseased arteries. Am J Cardiol 1993;71:3d-9d.
30. White CW. Clinical applications of Doppler coronary flow reserve measurements. Am J Cardiol 1993;71:10d-6d.
31. Kern MJ, Donohue TJ, Aguirre FV et al. Assessment of angiographically intermediate coronary artery stenosis using the Doppler flowire. Am J Cardiol 1993;71:26d-33d.
32. Segal J. Applications of coronary flow velocity during angioplasty and other coronary interventional procedures. Am J Cardiol 1993;71:17d-25d.
33. Serruys PW, De Bruyne B, Carlier S et al. Randomized comparison of primary stenting and provisional balloon angioplasty guided by flow velocity measurement. Doppler Endpoints Balloon Angioplasty Trial Europe (DEBATE) II Study Group. Circulation 2000;102:2930-7.
34. Nishida T, Di Mario C, Kern MJ et al. Impact of final coronary flow velocity reserve on late outcome following stent implantation. Eur Heart J 2002;23:331-40.
35. Albertal M, Regar E, Van Langenhove G et al. Value of coronary stenotic flow velocity acceleration in prediction of angiographic restenosis following balloon angioplasty. Eur Heart J 2002;23:1849-53.
36. Lotz J, Meier C, Leppert A, Galanski M. Cardiovascular flow measurement with phase-contrast MR imaging: basic facts and implementation. Radiographics 2002;22:651-71.
37. van Rossum AC, Galjee MA, Doesburg T, Hofman M, Valk J. The role of magnetic resonance in the evaluation of functional results after CABG/PTCA. Int J Card Imaging 1993;9 Suppl 1:59-69.
38. Galjee MA, van Rossum AC, Doesburg T, Hofman MB, Falke TH, Visser CA. Quantification of coronary artery bypass graft flow by magnetic resonance phase velocity mapping. Magn Reson Imaging 1996;14:485-93.
39. Hoogendoorn LI, Pattynama PM, Buis B, van der Geest RJ, van der Wall EE, de Roos A. Noninvasive evaluation of aortocoronary bypass grafts with magnetic resonance flow mapping. Am J Cardiol 1995;75:845-8.
40. Debatin JF, Strong JA, Sostman HD et al. MR characterization of blood flow in native and grafted internal mammary arteries. J Magn Reson Imaging 1993;3:443-50.
41. Sakuma H, Globits S, O'Sullivan M et al. Breath-hold MR measurements of blood flow velocity in internal mammary arteries and coronary artery bypass grafts. J Magn Reson Imaging 1996;6:219-22.
42. Brenner P, Wintersperger B, von Smekal A et al. Detection of coronary artery bypass graft patency by contrast enhanced magnetic resonance angiography. Eur J Cardiothorac Surg 1999;15:389-93.
43. Langerak SE, Kunz P, Vliegen HW et al. Improved MR flow mapping in coronary artery bypass grafts during adenosine-induced stress. Radiology 2001;218:540-7.
44. Langerak SE, Kunz P, Vliegen HW et al. Magnetic resonance flow mapping in coronary artery bypass grafts: a validation study with Doppler flow measurements. Radiology 2002;222:127-35.
45. Ishida N, Sakuma H, Cruz BP et al. Mr flow measurement in the internal mammary artery-to-coronary artery bypass graft: comparison with graft stenosis at radiographic angiography. Radiology 2001;220:441-7.
46. Bedaux WL, Hofman MB, Vyt SL, Bronzwaer JG, Visser CA, van Rossum AC. Assessment of coronary artery bypass graft disease using cardiovascular magnetic resonance determination of flow reserve. J Am Coll Cardiol 2002;40:1848-55.
47. Langerak SE, Vliegen HW, Jukema JW et al. Value of magnetic resonance imaging for the noninvasive detection of stenosis in coronary artery bypass grafts and recipient coronary arteries. Circulation 2003;107:1502-8.
48. Miller S, Scheule AM, Hahn U et al. MR angiography and flow quantification of the internal mammary artery graft after minimally invasive direct coronary artery bypass. AJR Am J Roentgenol 1999;172:1365-9.
49. Walpoth BH, Muller MF, Genyk I et al. Evaluation of coronary bypass flow with color-Doppler and magnetic resonance imaging techniques: comparison with intraoperative flow measurements. Eur J Cardiothorac Surg 1999;15:795-802.
50. Langerak SE, Vliegen HW, Jukema JW et al. Vein graft function improvement after percutaneous intervention: evaluation with MR flow mapping. Radiology 2003;228:834-41.

51. Salm LP, Langerak SE, Vliegen HW et al. Blood flow in coronary artery bypass vein grafts: volume versus velocity at cardiovascular MR imaging. Radiology 2004;232:915-20.
52. Salm LP, Bax JJ, Vliegen HW et al. Functional significance of stenoses in coronary artery bypass grafts Evaluation by single-photon emission computed tomography perfusion imaging, cardiovascular magnetic resonance, and angiography. J Am Coll Cardiol 2004;44:1877-82.
53. Tadamura E, Kudoh T, Motooka M et al. Use of technetium-99m sestamibi ECG-gated single-photon emission tomography for the evaluation of left ventricular function following coronary artery bypass graft: comparison with three-dimensional magnetic resonance imaging. Eur J Nucl Med 1999;26:705-12.
54. Germano G, Kiat H, Kavanagh PB et al. Automatic quantification of ejection fraction from gated myocardial perfusion SPECT. J Nucl Med 1995;36:2138-47.
55. Germano G, Erel J, Kiat H, Kavanagh PB, Berman DS. Quantitative LVEF and qualitative regional function from gated thallium-201 perfusion SPECT. J Nucl Med 1997;38:749-54.
56. Ascione R, Lloyd CT, Underwood MJ, Lotto AA, Pitsis AA, Angelini GD. Inflammatory response after coronary revascularization with or without cardiopulmonary bypass. Ann Thorac Surg 2000;69:1198-204.
57. Taggart DP. Biochemical assessment of myocardial injury after cardiac surgery: effects of a platelet activating factor antagonist, bilateral internal thoracic artery grafts, and coronary endarterectomy. J Thorac Cardiovasc Surg 2000;120:651-9.
58. Selvanayagam JB, Petersen SE, Francis JM et al. Effects of off-pump versus on-pump coronary surgery on reversible and irreversible myocardial injury: a randomized trial using cardiovascular magnetic resonance imaging and biochemical markers. Circulation 2004;109:345-50.
59. Steuer J, Bjerner T, Duvernoy O et al. Visualisation and quantification of peri-operative myocardial infarction after coronary artery bypass surgery with contrast-enhanced magnetic resonance imaging. Eur Heart J 2004;25:1293-9.
60. Selvanayagam JB, Kardos A, Francis JM et al. Value of delayed-enhancement cardiovascular magnetic resonance imaging in predicting myocardial viability after surgical revascularization. Circulation 2004;110:1535-41.
61. Albrechtsson U, Stahl E, Tylen U. Evaluation of coronary artery bypass graft patency with computed tomography. J Comput Assist Tomogr 1981;5:822-6.
62. Daniel WG, Dohring W, Stender HS, Lichtlen PR. Value and limitations of computed tomography in assessing aortocoronary bypass graft patency. Circulation 1983;67:983-7.
63. Brundage BH, Lipton MJ, Herfkens RJ et al. Detection of patent coronary bypass grafts by computed tomography. A preliminary report. Circulation 1980;61:826-31.
64. Guthaner DF, Brody WR, Ricci M, Oyer PE, Wexler L. The use of computed tomography in the diagnosis of coronary artery bypass graft patency. Cardiovasc Intervent Radiol 1980;3:3-8.
65. Godwin JD, Califf RM, Korobkin M, Moore AV, Breiman RS, Kong Y. Clinical value of coronary bypass graft evaluation with CT. AJR Am J Roentgenol 1983;140:649-55.
66. Wilson PC, Gutierrez O, Moss A. Early evaluation of coronary artery bypass grafts: CT or selective angiography. Eur J Radiol 1984;4:22-7.
67. Foster CJ, Sekiya T, Brownlee WC, Isherwood I. Computed tomographic assessment of coronary artery bypass grafts. Br Heart J 1984;52:24-9.
68. Muhlberger V, Knapp E, zur ND. Predictive value of computed tomographic determination of the patency rate of aortocoronary venous bypasses in relation to angiographic results. Eur Heart J 1990;11:380-8.
69. Kahl FR, Wolfman NT, Watts LE. Evaluation of aortocoronary bypass graft status by computed tomography. Am J Cardiol 1981;48:304-10.
70. Bateman TM, Gray RJ, Whiting JS et al. Prospective evaluation of ultrafast cardiac computed tomography for determination of coronary bypass graft patency. Circulation 1987;75:1018-24.
71. Stanford W, Rooholamini M, Rumberger J, Marcus M. Evaluation of coronary bypass graft patency by ultrafast computed tomography. J Thorac Imaging 1988;3:52-5.
72. Stanford W, Brundage BH, MacMillan R et al. Sensitivity and specificity of assessing coronary bypass graft patency with ultrafast computed tomography: results of a multicenter study. J Am Coll Cardiol 1988;12:1-7.
73. Tello R, Costello P, Ecker C, Hartnell G. Spiral CT evaluation of coronary artery bypass graft patency. J Comput Assist Tomogr 1993;17:253-9.
74. Ueyama K, Ohashi H, Tsutsumi Y, Kawai T, Ueda T, Ohnaka M. Evaluation of coronary artery bypass grafts using helical scan computed tomography. Catheter Cardiovasc Interv 1999;46:322-6.

75. Engelmann MG, von Smekal A, Knez A et al. Accuracy of spiral computed tomography for identifying arterial and venous coronary graft patency. Am J Cardiol 1997;80:569-74.
76. Yoo KJ, Choi D, Choi BW, Lim SH, Chang BC. The comparison of the graft patency after coronary artery bypass grafting using coronary angiography and multi-slice computed tomography. Eur J Cardiothorac Surg 2003;24:86-91.
77. Ko YG, Choi DH, Jang YS et al. Assessment of coronary artery bypass graft patency by multislice computed tomography. Yonsei Med J 2003;44:438-44.
78. Burgstahler C, Kuettner A, Kopp AF et al. Non-invasive evaluation of coronary artery bypass grafts using multi-slice computed tomography: initial clinical experience. Int J Cardiol 2003;90:275-80.
79. Willmann JK, Weishaupt D, Kobza R et al. Coronary artery bypass grafts: ECG-gated multi-detector row CT angiography--influence of image reconstruction interval on graft visibility. Radiology 2004;232:568-77.
80. Marano R, Storto ML, Maddestra N, Bonomo L. Non-invasive assessment of coronary artery bypass graft with retrospectively ECG-gated four-row multi-detector spiral computed tomography. Eur Radiol 2004;14:1353-62.
81. Nieman K, Pattynama PM, Rensing BJ, van Geuns RJ, de Feyter PJ. Evaluation of patients after coronary artery bypass surgery: CT angiographic assessment of grafts and coronary arteries. Radiology 2003;229:749-56.
82. Ropers D, Ulzheimer S, Wenkel E et al. Investigation of aortocoronary artery bypass grafts by multislice spiral computed tomography with electrocardiographic-gated image reconstruction. Am J Cardiol 2001;88:792-5.
83. Rumberger JA, Feiring AJ, Hiratzka LF et al. Quantification of coronary artery bypass flow reserve in dogs using cine-computed tomography. Circ Res 1987;61:117-23.
84. Tello R, Hartnell GG, Costello P, Ecker CP. Coronary artery bypass graft flow: qualitative evaluation with cine single-detector row CT and comparison with findings at angiography. Radiology 2002;224:913-8.
85. Dewey M, Lembcke A, Enzweiler C, Hamm B, Rogalla P. Isotropic half-millimeter angiography of coronary artery bypass grafts with 16-slice computed tomography. Ann Thorac Surg 2004;77:800-4.
86. Gurevitch J, Gaspar T, Orlov B et al. Noninvasive evaluation of arterial grafts with newly released multidetector computed tomography. Ann Thorac Surg 2003;76:1523-7.
87. Salm LP, Bax JJ, Jukema JW et al. Comprehensive assessment of patients after coronary bypass grafting by 16-detector row computed tomography. Am Heart J 2005;150:775-81.
88. Schlosser T, Konorza T, Hunold P, Kuhl H, Schmermund A, Barkhausen J. Noninvasive visualization of coronary artery bypass grafts using 16-detector row computed tomography. J Am Coll Cardiol 2004;44:1224-9.
89. Martuscelli E, Romagnoli A, D'Eliseo A et al. Evaluation of Venous and Arterial Conduit Patency by 16-Slice Spiral Computed Tomography. Circulation 2004;110:3234-8.
90. Herzog C, Dogan S, Diebold T et al. Multi-detector row CT versus coronary angiography: preoperative evaluation before totally endoscopic coronary artery bypass grafting. Radiology 2003;229:200-8.